A NON-BIOLOGICAL OPTION FOR SE REMOVAL BY PHOTOCATALYTIC REDUCTION OF SELENATE IN MINE-IMPACTED WATER CONTAINING HIGH CONCENTRATIONS OF SULFATE AND NITRATE

A. Holmes[1,4,5], K. Giesinger[2], J. Ye[3], E. Milan[6], A. Ngan[6] and F. Gu[1,4,6]

[1]University of Waterloo, Department of Chemical Engineering, Waterloo, Ontario
[2]University of Waterloo, Department of Environmental Engineering, Waterloo, Ontario
[3]University of Waterloo, Department of Environmental Sciences, Waterloo, Ontario
[4]Waterloo Institute of Nanotechnology, Waterloo, Ontario
[5]Geosyntec Consultants, Guelph, Ontario
[6]University of Toronto, Department of Chemical Engineering & Applied Chemistry, Toronto

ABSTRACT

Mine-impacted water (MIW) rich in selenium (Se) results from natural sources of water drainage, such as rain and snowmelt, infiltrating into waste rock piles and tailings on operating or abandoned mines. Dissolved Se is commonly found in its fully oxidized form, selenate, a highly bioavailable and mobile compound in the environment. The removal of selenate from MIW is desired, given its potential toxicity in aquatic ecosystems. MIW can contain varying concentrations of dissolved species, thus selective reduction of selenate is desired. In this study, we present the photocatalytic reduction of selenate over titanium dioxide (TiO_2) as a promising non-biological technique for selenate removal from mine-impacted water in order to remove Se from more than 600 $\mu g\ L^{-1}$ to below concentrations of 1 $\mu g\ L^{-1}$. For MIW treatment, the development of a process capable of removing selenate prior to biological denitrification process is desired, due to the numerous advantages achieved through removing Se from the biological process. This work sheds light on the mechanisms of selenate photocatalytic reduction and highlights the main drivers impacting the electron transfer process; information which can be used to build predictive models and engineer specialized solutions to achieve selective Se reduction under variable conditions.

KEYWORDS

Photocatalysis, selenium, mine-impacted water, TiO_2, advanced reduction process, titanium dioxide.

1.0 INTRODUCTION AND BACKGROUND

The introduction of selenium (Se) into aquatic ecosystems through anthropogenic activity is a rising global concern (Tan et al., 2016). Industrial activity such as the mining and smelting of metal ores, mining and combustion of coal, oil extraction and refining, and agricultural activities on seleniferous soils, disturb subsurface Se-rich deposits and introduce Se into surface aquatic environments (Hopkins et al., 2013; Schiavon and Pilon-Smits, 2017). Se is an essential nutrient for animals and humans, although it has a very narrow therapeutic window between deficiency and toxicity (El-Ramady et al., 2015). The most common soluble forms of Se found in the surface environment are the toxic Se oxyanions selenate (SeO_4^{2-}) and selenite (SeO_3^{2-}), which require reduction to the less soluble, biologically inert, elemental Se (Se^0) and selenides (M_nSe, H_2Se, etc.) for the removal from water.

Mine-impacted water (MIW) rich in Se is produced when natural sources of water drainage, such as rain and snowmelt, infiltrate into waste rock piles and tailings on an operating or abandoned mine. The composition of this water depends heavily on the geology of the underlying deposit and the overlying strata. MIW can contain varying concentrations of dissolved constituents from the underlying strata, such as sulfate, carbonate, nitrate, selenate and many dissolved metals (Nordstrom et al., 2015). Mine drainage can be acidic to alkaline, whereas areas high in carbonate content have near-neutral mine drainage (NMD) because H^+ ions produced from pyrite oxidation are neutralized by excessive carbonates naturally occurring in the overburden or added to the valley fill (Giam et al., 2018). Under these near-neutral conditions, dissolved Se is commonly found in its fully oxidized selenate form, a highly bioavailable and mobile compound in the environment (Fan et al., 2015).

Several conventional reduction processes can mitigate Se contamination of MIW including direct chemical amendment (Santos et al., 2015), reverse osmosis (Richards et al., 2011), adsorption (Rovira et al., 2008) and biological treatment options such as constructed wetlands (Martin et al., 2018) and bioreactors (Nancharaiah and Lens, 2015). Bioreactors have been successfully implemented as a method for Se removal from MIW on a pilot-and full-scale (Lenz et al., 2008; Luek et al., 2014). However, challenges remain for the disposal and stability of Se contaminated bioreactor sludge (Mal et al., 2017, 2016), microbial community start-up time and toxicity of effluents due to the possible production of organo-selenium compounds such as selenomethionine (LeBlanc and Wallschläger, 2016). Both O_2 and NO_3^- are more energetically favourable electron acceptors than Se oxyanions and thus, NO_3^- reduction can occur prior to selenate reduction in anaerobic bioreactors ($E'_{0,\,O_2/H_2O}$= +0.81 V > $E'_{0,\,NO_3^-/N_2}$= +0.75 V > $E'_{0,\,SeO_4^{2-}/SeO_3^{2-}}$= +0.48 V > $E'_{0,\,SeO_3^{2-}/Se^0}$= +0.21 V > $E'_{0,\,SO_4^{2-}/SO_3^{2-}}$= -0.516 V (Y. V. Nancharaiah and Lens, 2015)). For MIW treatment, the development of a process capable of removing selenate prior to biological denitrification process is desired due to the numerous advantages achieved by removing Se from the biological process.

Photocatalytic reduction on semiconductor materials, mainly titanium dioxide (TiO_2), has shown great potential for removal of several contaminants of interest such as nitrate (Marks et al.,

2016; Shaban et al., 2016; Sun et al., 2016), nitrite (Luiz et al., 2012), chromate (Choi et al., 2017), bromate (Xiao et al., 2017), perchlorate (Jia et al., 2016) selenite (Nguyen et al., 2005) and selenate (Tan et al., 2003a; Leshuk et al., 2018; Holmes and Gu, 2016). Upon irradiation of a photocatalyst with high-energy light, electrons are excited into the conduction band (e_{cb}^-) and electron holes form in the valence band (h_{vb}^+). An electron acceptor capturing the e_{cb}^- is reduced while an electron donor reacting with the h_{vb}^+ is oxidized, whereas the semiconductor catalyst remains unchanged. In the case of Se removal, the photogenerated e_{cb}^- can reduce SeO_4^{2-} to Se^0 or H_2Se under the right conditions. Utilization of an electron hole scavenger, an easily oxidizable organic material, such as methanol, ethanol, or formic acid, can limit the recombination of the e_{cb}^--h_{vb}^+ pairs, thus markedly increasing the efficacy of reduction, through mediating the transfer of electrons to selenate to reduce the oxidation state of Se.

Herein, the authors investigate the photocatalytic reduction of selenate over TiO_2 in MIW; focusing on various factors that impact the kinetics of reduction including pH, temperature, dissolved oxygen, electron hole scavenger type and concentration. We report for the first time that photocatalytic reduction can selectively remove Se from MIW containing many other competing ions in the complex real water source. As a result, it may be advantageous to couple photocatalytic Se removal with biologic nitrate reduction to meet the effluent limit guidelines for both Se and nitrate. The removal of Se prior to biological nitrate removal has numerous advantages: (1) no Se contamination of the bioreactor sludge; (2) biological process can be designed for denitrification only; (3) generation of a recoverable, concentrated Se-containing residual; (4) no production of organo-Se compounds and (5) compatible electron donors can be used for both photocatalytic and biological processes. The primary goal of this work is to understand the conditions which optimize the removal of selenate in MIW. Given that treatment of MIW is unique depending on the water source, parameters for Se treatment were independently investigated to understand the kinetic effects of varying parameters and envision a photocatalytic Se removal process within an overall water treatment system.

2.0 MATERIALS AND METHODS

2.1 Materials

Mine-impacted water (MIW) was received from an operating mine in North America and stored at 4 °C in the dark. Titanium dioxide nanoparticles (Aeroxide P25, ~10-50 nm particle diameter, 55 m^2 g^{-1} surface area, Acros) were used as received. P25 TiO_2 nanoparticles have been extensively studied and characterized in the literature and are often used as a benchmark photocatalyst. Formic acid (ACS reagent, 97%, Alfa Aesar) was used as an electron hole scavenger. Sodium selenate (<0.1% impurities, BioXtra, Sigma-Aldrich), calcium sulphate (anhydrous, ACS reagent >96%, Sigma-Aldrich), sodium chloride (reagent grade, Sigma-Aldrich), sodium nitrate (>99%, ReagentPlus, Sigma-Aldrich), hydrochloric acid (37%), and sodium hydroxide (ACS grade, Sigma-Aldrich) were used to simulate MIW for more controlled experiments.

2.2 Photocatalytic reduction of selenate experiments

The photocatalytic reactor apparatus consists of an air tight stainless-steel reactor vessel of 1.0 L capacity with a quartz window through which UV was irradiated onto the mixing TiO_2 suspension. TiO_2 nanoparticles (0.2 g/L) were stirred into 400 mL of MIW in a polytetrafluoro-ethylene (PTFE) beaker (76 mm diameter) along with an electron hole scavenger for the reduction reaction. The air-tight stainless-steel vessel with a quartz window was purged by bubbling N_2 gas throughout the reaction to remove any H_2Se gas generated and flowing through two subsequent liquid scrubbers of $CuSO_4$ and NaOH, respectively (Sanuki et al., 1999; Tan et al., 2003b). The TiO_2-MIW suspension was stirred in the dark under a N_2 gas purge for 1 h to attain adsorption-desorption equilibrium of the inorganics with the TiO_2 surface as well as to remove dissolved oxygen, and then placed in the photoreactor and exposed to UV light while stirring. Filtered and unfiltered 5 mL aliquots were sampled periodically to measure the dissolved and total Se concentrations, respectively. The reactor vessel was exposed to UV light using a UVA fluorescent bulb that was filtered to only supply UVA (λ = 365 nm) light (Blak Ray B-100A). The UV intensity (I_{UV}) at the height of the solution-air interface within the vessel was 11.03 mW/cm^2 (measured with a UVA/B light meter, Sper Scientific, NIST certified calibration). The energy dosage was varied instead of operating time to make our results comparable with other photocatalytic studies. The energy reported on the x-axis, in units of kWh/m^3, is the received energy by the suspension, not the electrical energy required by the UV lamp. Due to low conversion efficiencies of medium pressure UV lamps the required energy will be more depending on the conversion efficiency of the UV lamp being utilized in the reactor set-up.

2.3 Analysis

Se concentration was determined in accordance with the U.S. EPA suggested Se determination technique (APHA 2009, Method 3114B/C) using Hydride Generation Inductively Coupled Plasma Optical Emission Spectroscopy (HG-ICP-OES, Teledyne Prodigy ICP and Cetac HGX-200 advanced membrane hydride generation system, LOD = 1 µg L^{-1}). Both dissolved and total Se were determined by HG-ICP-OES following acid digestion protocol U.S. EPA Method 3050B (U.S. EPA, 1996). The insoluble Se fraction (considered to be elemental Se) present in the water was calculated by the difference of total and dissolved Se concentrations. Gaseous H_2Se was calculated from the difference between the initial total Se in the water and total Se in the TiO_2 suspension after UV exposure. Based on several past studies on photocatalytic reduction of selenate on TiO_2 (Nguyen et al., 2005; Sanuki et al., 1999; Tan et al., 2003a), the gaseous Se species is assumed to be H_2Se, although the direct identification of gaseous Se species is a challenging task (Kot and Namieśnik, 2000; Uden, 2002). Analytical chemistry of Se is currently a developing field with researchers looking into new and improved approaches to measure gaseous and solid Se species concentrations (Santos et al., 2015).

Dissolved oxygen content was determined through the use of a lab-bench probe (Thermo Scientific Orion Star A213 benchtop meter). Total organic carbon (TOC, APHA 5310B,

combustion temperature 800 °C), chemical oxygen demand (COD, APHA 5220D), biochemical oxygen demand (BOD, APHA 5210B), anion concentration by ion chromatography (bromide, chloride, fluoride, nitrate, nitrite and sulfate, EPA 300.1), total ammonia (Watson et al., 2005), speciated alkalinity (as $CaCO_3$, EPA 310.2), and total and dissolved metals by inductively coupled plasma mass spectrometry (ICPMS, EPA 200.2/6020A and APHA 3030B/6020A) were measured according to standard methods by ALS Environmental (Calgary, AB, Canada), a laboratory certified by the Canadian Association for Laboratory Accreditation (CALA) according to international standards (ISO 17025). Total and dissolved Se concentrations measured at the University of Waterloo were confirmed by ALS Environmental on a number of analytical checks.

3.0 RESULTS AND DISCUSSION

3.1 Reduction of selenate to solid Se^0 and gaseous H_2Se in MIW

Photocatalytic experiments were conducted to investigate the speciation of Se during the Se removal in MIW to better understand the mechanism of Se removal. Figure 1 presents the effect of incident UVA energy on SeO_4^{2-}, Se^0 and H_2Se concentrations resulting from photoreduction of selenate in MIW over TiO_2. The photocatalytic reduction of SeO_4^{2-} undergoes a two-step reaction outlined in eq. 1 & 2, with the reduction of SeO_4^{2-} to Se^0 followed by further reduction to H_2Se.

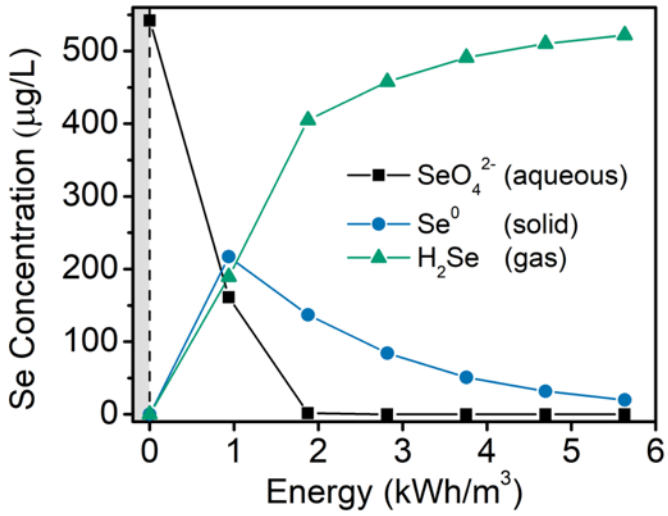

Figure 1. Effect of incident UVA energy on the photocatalytic reduction of selenate in mine impacted water over TiO_2 using formic acid as an electron hole scavenger. (Reaction conditions: 300 mg L^{-1} formic acid, 0.2 g/L TiO_2, 37 °C, pH 4.5)

$$SeO_4{}^{2-}{}_{(aq)} + 8H^+ + 6e^-_{cb} \xrightarrow{k_1} Se^0{}_{(s)} + 4H_2O \quad (E^0 = 0.5\ V\ vs.\ SHE) \tag{1}$$

$$Se^0{}_{(s)} + 4H^+ + 2e^-_{cb} \xrightarrow{k_2} H_2Se_{(g)} \quad (E^0 = -0.6\ V\ vs.\ SHE) \tag{2}$$

Both products of selenate reduction, H_2Se and Se^0, are removed from the MIW solution through the gas phase with N_2 purging and from the solid phase by filtering the catalyst from the suspension, respectively. The photocatalytic reduction of Se in MIW was able to lower concentration to less than 2 $\mu g\ L^{-1}$ Se in the treated effluent after 2.0 kWh/m^3 of incident energy. At lower energies, nearly equal amounts of H_2Se and Se^0 are produced. Once the selenate is largely removed from solution, the solid Se^0 starts to convert to gaseous H_2Se and is then removed from the system. The colour of the catalyst that is filtered out of solution changes from its native white (colour of TiO_2) to red-pink (colour of solid elemental Se) during the first stage of reduction between 0 and 2.0 kWh/m^3, and then slowly changes back to white at higher energies. Thus, during the first stage of reduction selenate is being reduced to elemental Se (eq. 1), which is being deposited onto the surface of TiO_2. After near exhaustion of selenate from solution, at around 2.0 kWh/m^3, the elemental Se on the surface of TiO_2 is further reduced to H_2Se gas and removed from solution (eq. 2).

3.2 Effect of electron hole scavenger

The effects of various organic electron hole scavengers (methanol, ethanol, acetic acid, glycerol and formic acid) were investigated to determine the optimal photocatalytic reduction rates of selenate in MIW. As shown in Figure 2, the use of 300 mg L^{-1} formic acid achieves the fastest Se removal rate. Se photoreduction was achieved with all tested electron hole scavengers with increasing Se removal rates in accordance to the following order: acetic acid < ethanol < methanol < glycerol < formic acid. All experiments were initially completed at a nominal concentration of 300 mg L^{-1}, however in the instance of acetic acid, ethanol and methanol the photoreductions were quite slow and their concentrations were increased to 800 mg L^{-1} to better characterize the reduction kinetics.

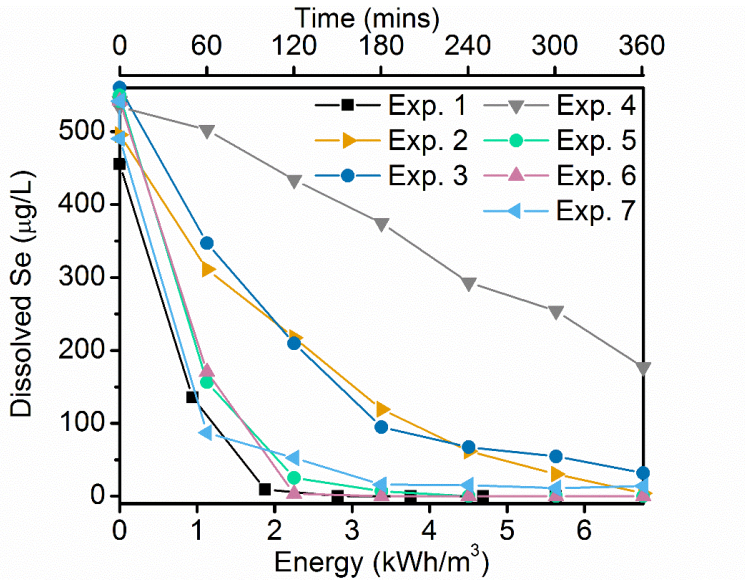

Figure 2. Selenate reduction in MIW while using various electron hole scavenger types and concentrations. (1) 300 mg L^{-1} formic acid, (2) 800 mg L^{-1} methanol, (3) 800 mg L^{-1} ethanol, (4) 800 mg L^{-1} acetic acid, (5) 300 mg L^{-1} acetic acid and 100 mg L^{-1} formic acid, (6) 100 mg L^{-1} formic acid, and (7) 800 mg L^{-1} glycerol. (Reaction conditions: 0.2 g/L TiO_2, 37 °C, pH 4.5)

Previous studies investigating the effect of organic hole scavengers on the photocatalytic reduction of selenium oxyanions, found a similar trend for the order of increasing Se removal rates with electron hole scavengers of ethanol < methanol < formic acid (Tan et al., 2003a). Reasons for formic acid being the most efficient hole scavenger are its ability to compete with the selenate ion, and most likely sulfate ions, for the TiO_2 surface sites, its rapid mineralization and ability to form reducing radicals, such as $CO_2^{\bullet -}$. Tan et al. reported no Se photoreduction with the use of acetic acid, whereas our study showed acetic acid capable of reducing some selenate (Exp. 4 in Figure 2). The experiments were done under very similar operating conditions, with the exception of a higher concentration of Se in the water being treated (20 ppm Se(VI)) in the work done by Tan et al. It is likely that under excess concentration of selenate, acetic acid is incapable of competing for adsorption sites on the surface of TiO_2 and thus rendered ineffective at scavenging electron holes.

Photocatalytic reduction can selectively remove Se from MIW containing many other competing ions in the complex real water source (as shown in Figure 3c & f). As a result, it may be advantageous to couple photocatalytic Se removal with biologic nitrate reduction to meet the effluent limit guidelines for both Se and nitrate. This offers many advantages over conventional biological reduction of both selenate and nitrate, namely no formation of organic selenium species, such as selenomethionine and other discrete organic Se species with a potentially increased bioavailability (LeBlanc and Wallschläger, 2016). During selective Se removal in the presence of nitrate, most of the organic hole scavenger remains in solution after Se is largely removed (as shown in Figure 3c & f). Therefore, the residual organic scavenger can subsequently be utilized in downstream denitrification. The denitrification process would convert the electron donor to CO_2

in the final biological step so no residual organics species would have to be removed further downstream.

The primary electron donors used for biological denitrification are acetic acid, glycerol, methanol and ethanol (Bill et al., 2009; Strong et al., 2011). Formic acid has been used as an electron donor in the denitrification process as well, although bioreactor acclimation is required in order to ensure the microbes can effectively utilize formic acid as a carbon source (Li et al., 2015; Nishimura et al., 1980; R. H. Gerber, 1986). Figure 3 compares the reduction of selenate and production of Se^0 and H_2Se in MIW when using 300 mg L^{-1} of either formic acid or glycerol. Both glycerol and formic acid provide selective Se removal in the presence of nitrate and sulfate in MIW, leaving the nitrate and sulfate in solution. Inspection of Figure 3b & e shows the removal of aqueous selenate is faster with formic acid, due to a larger proportion of solid Se^0 generation. The actual amount of H_2Se generation for both trials is very similar, with the total amount of Se remaining in solution ($SeO_4^{2-}{}_{(aq)}$ + $Se^0{}_{(s)}$) nearly equal for both formic acid and glycerol. It is postulated that formic acid generates more Se solid due to the fact that it adsorbs more favorably to the surface of TiO_2 through electrostatic forces, whereas glycerol adsorbs weakly through van der Waals forces and hydrogen bonding.

Aside, from a higher selenate reduction rate constant, the addition of formic acid also leads to a lower pH. Lower pH leads to faster selenate photocatalytic reduction. The addition of HCl for pH reduction can be done followed by an addition of NaOH to raise the pH after treatment. However, this method adds to the already elevated total dissolved solids (TDS) in the treated water and is unfavorable. The presence of formic acid reduces pH but is a dissolved species that will be removed in the subsequent biological reduction of nitrate. Thus, formic acid is considered a suitable electron donor for this photocatalytic process.

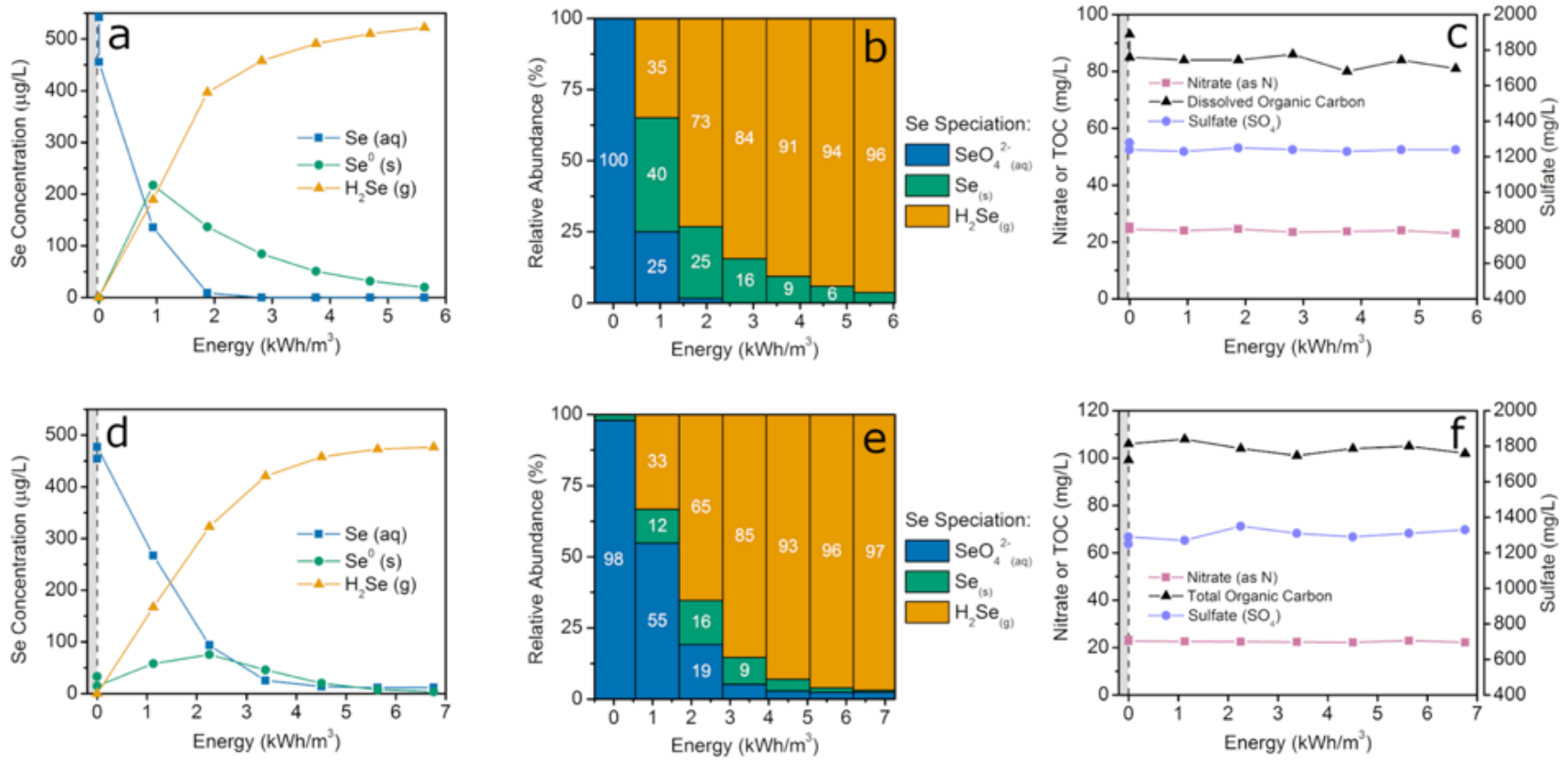

Figure 3. Selenate reduction in MIW using 300 mg L^{-1} formic acid (a-c) and glycerol (d-f) as electron hole scavenger. (a/d) Se mass balance, (b/e) Se percentage speciation, and (c/f) Concentrations of nitrate, sulfate and organic carbon during selenate photocatalytic reduction. (Reaction conditions: 0.2 g/L TiO_2, 37 °C, pH 4.5)

To ensure that the use of electron hole scavengers is scalable to a larger industrial process, industrial grade sources of both glycerol and formic acid were acquired and tested. An economical source of glycerol from Environmental Operating Solutions, Inc. called MicroC4200, which contains 72 wt% glycerol was tested. Comparison of industrial glycerol from MicroC4200 to lab grade glycerol. The lab grade glycerol shows faster selenate photocatalytic reduction kinetics, likely due to the presence of close to 5 wt% NaCl in MicroC4200, which could inhibit the adsorption of selenate onto TiO_2 through charge screening of the electrostatic adsorption. The increase of ionic strength in solution can also lead to increased aggregation of TiO_2 reducing catalytic surface area, following DLVO theory (Hotze et al., 2010). A source of industrial grade formic acid was acquired and compared to the results with lab grade formic acid (Figure 4). The industrial grade formic acid and lab grade formic acid exhibit similar selenate removal kinetics as well as the selectivity between solid Se^0 and gaseous H_2Se production.

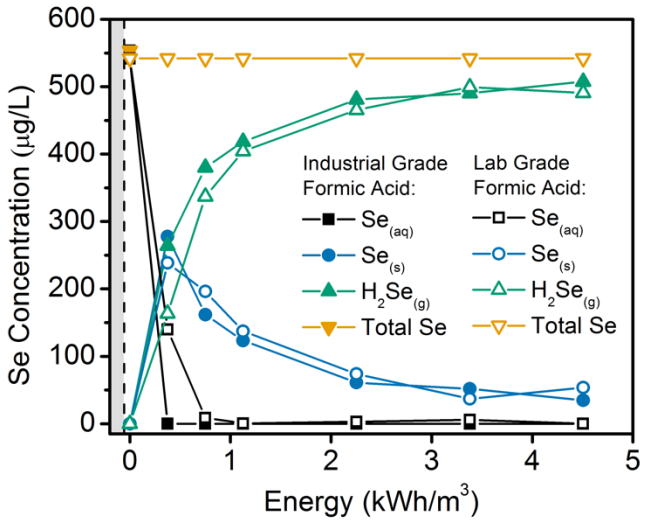

Figure 4. Comparison of Se speciation while using lab grade formic acid from Sigma-Aldrich vs. industrial grade formic acid sourced from Quadra Chemicals used as electron hole scavengers during the photocatalytic reduction of selenate in MIW.

3.3 Effect of pH

The acidity or basicity of mine-impacted water drainage depends heavily on the geology of the underlying deposit and the overlying strata (U.S. EPA, 2011). Mine drainage is neutral to alkaline in some areas in North America because H^+ ions produced from pyrite oxidation are neutralized by carbonates naturally occurring in the overburden or added to the valley fill (Giam et al., 2018; Petty et al., 2010). As a result of the high carbonate concentrations, the incoming pH of mine-impacted water tends to be neutral to alkaline, which influences the photocatalytic reduction process significantly.

pH is known to highly influence the photoreduction process of selenate due to the outer-sphere complexes formed between TiO_2 and the selenate anion (Jordan et al., 2011). Given the

point-of-zero charge (PZC) of TiO_2 (PZC = 5.6-6.2 (Jiang et al., 2008; Suttiponparnit et al., 2010)), the zeta potential is positive at pHs under ~6. Under these acidic conditions, anionic selenate is electrostatically attracted to the positively charge TiO_2 surface. This attraction contributes to a stronger outer-sphere adsorption of selenate, which is a key first step in the photocatalytic reduction process. Thus, we studied the effect of pH on the photocatalytic reduction of selenate in MIW. Experiments were conducted under controlled pH conditions, using the same concentration of electron hole scavenger for each trial, followed by pH adjustment with either NaOH or HCl to maintain the desired pH throughout the entire experiment. Figure 5 presents the experimental results of this study, showing that the extent of selenate reduction decreases with increasing pH (pH range 3.5-6.6). When the pH of the solution is raised above the PZC of TiO_2, the reaction markedly slows, resulting from the inhibition of electrostatic-mediated outer-sphere adsorption of selenate onto TiO_2.

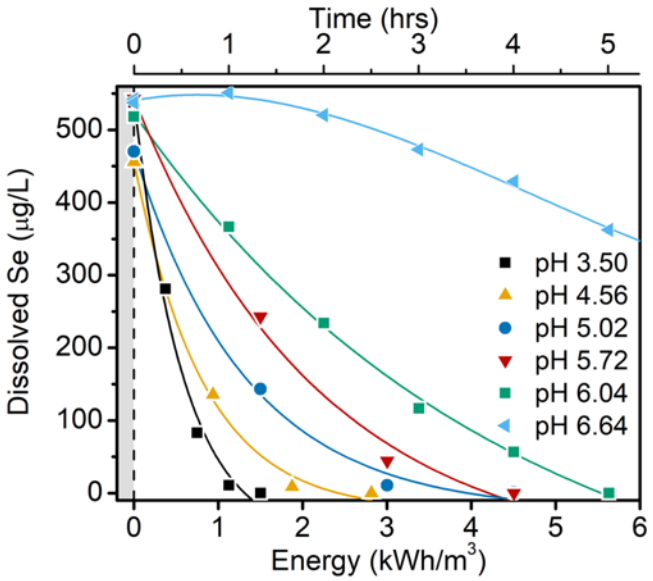

Figure 5. Selenate removal from mine impacted water using formic acid as an electron donor under varying pH. (Reaction conditions: 300 mg L^{-1} formic acid, 0.2 g/L TiO_2, 37 °C)

Experiments without pH control were also conducted at different initial pH of the solution. Under these conditions, the reduction of selenate was completely inhibited above an initial pH of 5.0, likely due to the pH rise during the photoreduction. At a pH_0 of 5.0, photoreduction begins in a similar manner to that presented in Figure 5; however after 1 kWh/m^3 of UV exposure the reaction suddenly stops and no more Se is removed from solution. At a pH_0 of 5.5, photoreduction fails to remove any Se from the MIW. These experiments suggest that the pH of the solution increases during either dark adsorption or UV exposure. Control experiments were conducted to determine the nature of pH variation throughout the reduction of selenate. When the electron donor formic acid is added at concentrations of 300 and 100 mg/L, initial pH of the MIW drops from ~8.5 to 4.5 and 5.5, respectively. An additional amount of HCl was then added to the solution of 100 mg/L formic acid to bring the pH_0 to 4.5 and maintain similar initial reaction kinetics. The photocatalytic reduction of selenate proceeded similarly to when pH was controlled, although the

pH increased substantially more in the case of 100 mg/L formic acid. The pH increase is likely due to the abstraction of H^+ ions from solution for the production of reduction products such as H_2Se. The oxidation of formic acid to CO_2 is minimal throughout the reaction (< 3%), as indicated by TOC concentration measurements before and after the reaction and thus not likely a major cause of increasing pH.

3.4 Effect of temperature

Experiments were completed to investigate the effects of temperature on the reaction kinetics for the reduction of selenate in MIW. The Arrhenius plot of the apparent first-order rate constants (inset of Figure 6) was used to calculate an apparent activation energy (E_{aa}) of 31.83 ± 7.07 kJ mol^{-1} for the reduction of selenate in MIW, using formic acid as an electron donor. The conclusion from our previous work is that the high TDS or ionic strength of the wastewater (primarily from Ca^{2+} and SO_4^{2-}) leads to a higher apparent activation energy of the photocatalytic reaction. Thermally accessible defects in photo-deposited $Se_{(s)}$ cause greater electron excitation at higher temperatures, while high levels of Ca^{2+} and SO_4^{2-} contribute to a high E_{aa} caused by bend bending at the electrolyte-catalyst interface.

Total mass balances were completed during experiments in order to investigate the role temperature plays on the generations of, $Se_{(s)}$ and $H_2Se_{(g)}$. Table 1 reports maximum % solid Se generated and the solid Se selectivity throughout the photoreduction of selenate from MIW at four temperature (12 °C, 27 °C, 37 °C and 47 °C). Selectivity of solid Se product is calculated by:

$$S\left(Se^0_{(s)}\right)_t = \frac{\left[Se^0_{(s)}\right]_t}{\left[SeO_4^{-2}\right]_0 - \left[SeO_4^{-2}\right]_t} \quad (3)$$

The only possible reduction products are $Se_{(s)}$ and $H_2Se_{(g)}$, thus the selectivity of $H_2Se_{(g)}$ is simply calculated as $1 - S\left(Se^0_{(s)}\right)_t$. Table 1 highlights the maximum percent of $Se_{(s)}$ generation (calculated by $[Se_{(s)}]_t$ / $[Se_{Total}]_0$) during the run and the initial selectivity of solid Se. At lower temperatures, the selectivity of the solid Se product is much higher and more $Se_{(s)}$ is generated during the reaction. $Se_{(s)}$ is an intermediate product, which is further reduced to $H_2Se_{(g)}$, hence at lower temperatures this second reaction (Outlined in Eq. 1) is inhibited. The kinetics of the overall reaction is slower at lower temperatures leading to increased reaction times needed to achieve similar Se removal.

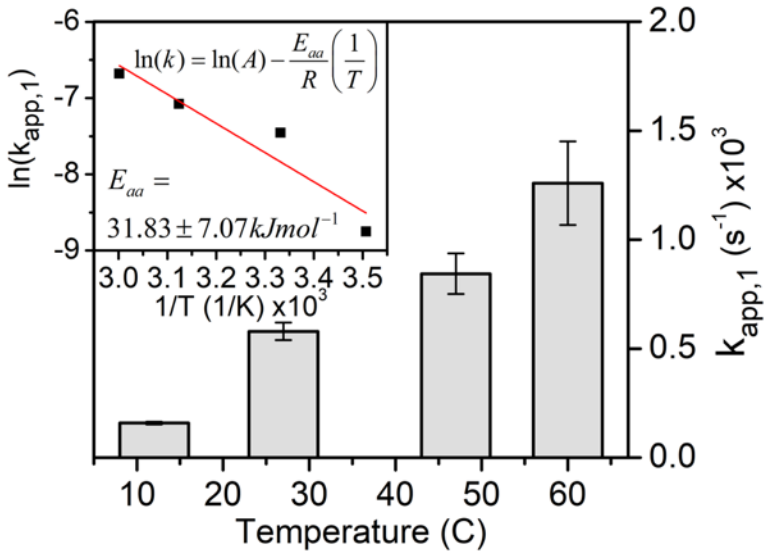

Figure 6. Apparent first-order rate constant as a function of reaction temperature for the photocatalytic reduction of selenate in MIW with inset Arrhenius plot. (Reaction conditions: 300 mg L^{-1} formic acid, 0.2 g/L TiO_2, pH 4.5).

Table 1. Maximum $Se_{(s)}$ generation and initial selectivity of $Se_{(s)}$ with varying temperatures.

Temperature (°C)	Maximum $Se_{(s)}$ Generation	Average $\mathbf{S(Se^0_{(s)})_t}$
12	56.3 %	78.9 %
27	38.8 %	45.2 %
37	40.0 %	53.4 %
47	32.6 %	44.5 %

Within Se-TiO_2 photocatalytic systems, the large temperature dependence arises for two main reasons: intrinsic semiconductor properties and solution film mass transport associated with adsorption of reactants and desorption of products. To explain the former, the photodeposited Se^0 contains thermally accessible defects which reduce the bandgap of Se, allowing for greater electron excitation at higher temperatures (Kasap et al., 2015). The simultaneous inhibition of the overall reduction reaction and the increase in selectivity to $Se_{(s)}$ suggests that the reduction of $Se_{(s)}$ to $H_2Se_{(g)}$ is a bottleneck at lower temperatures. This result reinforces the theory of thermally accessible defects within amorphous Se which allow the second reaction and therefore the entire selenate reduction to proceed at a faster rate at higher temperatures. A threshold temperature appears to occur between 12°C and 27°C, above which an increase in temperature has much less of an effect on the reaction rate.

3.5 Effect of dissolved oxygen (DO)

Selenate removal from MIW via photocatalytic reduction on TiO_2 was compared for five different durations of nitrogen (N_2) purge of 0, 5, 10, 20 and 60 minutes, which resulted in initial dissolved oxygen (DO) concentrations of 6.3, 5.0, 3.8, 3.3 and 2.7 mg/L, respectively. As shown in Figure 7, selenate removal by photocatalytic reduction required 3.3 mg/L DO or lower to achieve effective Se removal. O_2 is known to react with photogenerated electrons in the conduction band of TiO_2, forming superoxide radicals ($O_2^{\bullet-}$), and at low pH the protonated hydroperoxyl radical ($^{\bullet}O_2H$), a very powerful oxidant (Turolla et al., 2015). The $^{\bullet}O_2H$ radical can oxidize elemental $Se_{(s)}$ back to selenate, greatly inhibiting the reaction. Throughout the photocatalytic reaction DO is decreasing, indicating the conversion of molecular oxygen into redox byproducts. During the 5 and 10 min N_2 purge experiments the DO concentrations initially exceeds the required 3.3 mg/L. However, as the UV exposure progresses, the DO in both experiments drops down to 2.6 and 2.5 mg/L, respectively. Although the DO dipped below the threshold concentration to initiate the selenate reduction reaction, the reaction still did not proceed. It is postulated that the produced $^{\bullet}O_2H$ generated under the initial UV exposure, is responsible for an oxidizing environment which inhibits selenate reduction regardless of final DO concentration.

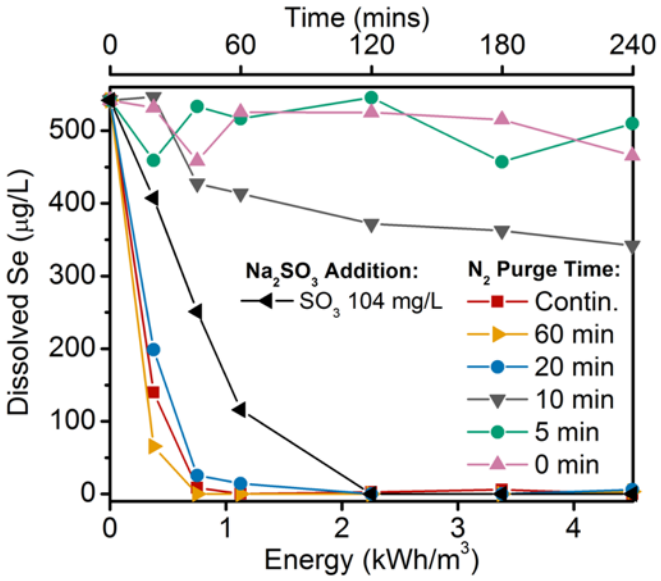

Figure 7. Selenate removal from mine impacted water using formic acid as an electron donor with varying N_2 purge times which result in varying concentrations of dissolved oxygen or the addition of the oxygen scavenger, Na_2SO_3. (Reaction conditions: 300 mg L^{-1} formic acid, 0.5 g/L TiO_2, 37 °C, pH 4.5)

N_2 purging is an effective method of DO removal in a laboratory environment but is not practical for many large industrial applications. Industrial scale DO removal techniques include membrane contactors, cold water vacuum deaeration, hot water stripping deaeration and the use

of oxygen scavengers (Pabby et al., 2008). The most commonly used oxygen scavenger for low pressure systems is sodium sulfite (Na_2SO_3) which reacts with low concentrations of oxygen to form sodium sulfate (Na_2SO_4). An experiment was conducted to demonstrate selenate reduction in MIW utilizing Na_2SO_3. A dose of 104 mg/L Na_2SO_3 was added to achieve an initial DO level of 2.2 mg/L, sufficiently below the concentration threshold of 3.3 mg/L determined previously through the N_2 purge experiments. The reduction of selenate in this trial was slower than that during the 20 and 60 min N_2 purge times, even though the initial DO concentrations were much lower. This is likely a result of the interaction between TiO_2 and sodium sulfite and sulfate prior to UV exposure. Both sulfite and sulfate are known to adsorb effectively to TiO_2 surfaces and compete for adsorption sites with selenate (Sheng et al., 2013; Yang et al., 2013).

4.0 CONCLUSIONS

The photocatalytic reduction on TiO_2 is a promising non-biological technique for selenate removal from MIW in order to remove Se below 1 μg L^{-1}. Selenate is reduced to solid elemental Se (Se^0) and gaseous hydrogen selenide (H_2Se) in subsequent heterogeneous photocatalytic reactions. The product selectivity towards solid Se^0 versus gaseous H_2Se is influenced by many factors, including temperature and electron hole scavenger. Regardless of the high sulfate, nitrate, and carbonate concentrations and the presence of various trace metals contained in MIW the photocatalytic reaction was able to reduce selenate under different reaction conditions from >500 μg L^{-1} Se to < 1 μg L^{-1}. Below the point of zero charge of TiO_2 (PZC_{TiO2}= 5.6-6.2), faster kinetics are achieved at lower pHs due to the positive zeta potential of the catalyst surface and increased electrostatic attraction and outer-sphere adsorption of selenate. The highest pH able to achieve significant Se removal was pH 6.04 while the best kinetics were observed at pH 3.50. Temperature plays a major role in the reduction of selenate, which has an activation energy of 31.83 kJ mol^{-1}. Higher temperatures lead to higher selectivity toward H_2Se as well as faster selenate removal kinetics. The reaction is inhibited in the presence of dissolved oxygen (DO). The removal of DO prior to selenate removal was successfully achieved through N_2 purging to strip O_2 and the use of an oxygen scavenger, Na_2SO_3, which is a more scalable and practical DO removal alternative.

The impact of various electron hole scavengers on the kinetics of selenate photocatalytic reduction was investigated. Se photoreduction was achieved with all tested electron hole scavengers with Se removal rates increasing in the following order: acetic acid < ethanol < methanol < glycerol < formic acid. Marginal differences to the selectivity of Se^0 vs. H_2Se were observed between glycerol and formic acid, which are both selective towards H_2Se generation under the conditions studied. The photocatalytic removal of selenate appears to be selective, leaving nitrate and sulfate essentially unreduced, a phenomenon which is attractive due to the numerous advantages presented by Se removal prior to denitrification. As a result, it may be advantageous to couple photocatalytic Se removal with biologic nitrate reduction, in order to meet the effluent limit guidelines for both Se and nitrate. During the selective Se removal in the presence of nitrate, the majority of the organic hole scavenger remains in solution after the Se is fully removed and may then be used for the downstream denitrification as an electron donor.

REFERENCES

Arakawa, H., Sayama, K., 2000. Solar hydrogen production. Significant effect of Na2CO3 addition on water splitting using simple oxide semiconductor photocatalysts. Catal. Surv. Jpn. 4, 75–80. https://doi.org/10.1023/A:1019096323694

Bill, K.A., Bott, C.B., Murthy, S.N., 2009. Evaluation of alternative electron donors for denitrifying moving bed biofilm reactors (MBBRs). Water Sci. Technol. J. Int. Assoc. Water Pollut. Res. 60, 2647–2657. https://doi.org/10.2166/wst.2009.622

Choi, J., Lee, H., Choi, Y., Kim, S., Lee, Seokheon, Lee, Seunghak, Choi, W., Lee, J., 2014. Heterogeneous photocatalytic treatment of pharmaceutical micropollutants: Effects of wastewater effluent matrix and catalyst modifications. Appl. Catal. B Environ. 147, 8–16. https://doi.org/10.1016/j.apcatb.2013.08.032

Choi, Y., Koo, M.S., Bokare, A.D., Kim, D., Bahnemann, D.W., Choi, W., 2017. Sequential Process Combination of Photocatalytic Oxidation and Dark Reduction for the Removal of Organic Pollutants and Cr(VI) using Ag/TiO2. Environ. Sci. Technol. 51, 3973–3981. https://doi.org/10.1021/acs.est.6b06303

El-Ramady, H., Abdalla, N., Alshaal, T., Domokos-Szabolcsy, É., Elhawat, N., Prokisch, J., Sztrik, A., Fári, M., El-Marsafawy, S., Shams, M.S., 2015. Selenium in soils under climate change, implication for human health. Environ. Chem. Lett. 13, 1–19. https://doi.org/10.1007/s10311-014-0480-4

Fan, J., Wang, R., Hu, H., Huo, G., Fu, Q., Zhu, J., 2015. Transformation and Bioavailability of Selenate and Selenite Added to a Nicotiana tabacum L. Planting Soil. Commun. Soil Sci. Plant Anal. 46, 1362–1375. https://doi.org/10.1080/00103624.2015.1033544

Fotiou, T., Triantis, T.M., Kaloudis, T., Hiskia, A., 2015. Evaluation of the photocatalytic activity of TiO2 based catalysts for the degradation and mineralization of cyanobacterial toxins and water off-odor compounds under UV-A, solar and visible light. Chem. Eng. J., Photocatalysis for disinfection and removal of contaminants of emerging concern 261, 17–26. https://doi.org/10.1016/j.cej.2014.03.095

Giam, X., Olden, J.D., Simberloff, D., 2018. Impact of coal mining on stream biodiversity in the US and its regulatory implications. Nat. Sustain. 1, 176. https://doi.org/10.1038/s41893-018-0048-6

Holmes, A.B., Gu, F.X., 2016. Emerging nanomaterials for the application of selenium removal for wastewater treatment. Environ. Sci. Nano 3, 982–996. https://doi.org/10.1039/C6EN00144K

Hopkins, R.L., Altier, B.M., Haselman, D., Merry, A.D., White, J.J., 2013. Exploring the legacy effects of surface coal mining on stream chemistry. Hydrobiologia 713, 87–95. https://doi.org/10.1007/s10750-013-1494-9

Hotze, E.M., Phenrat, T., Lowry, G.V., 2010. Nanoparticle aggregation: challenges to understanding transport and reactivity in the environment. J. Environ. Qual. 39, 1909–1924.

Jia, Y., Ye, L., Kang, X., You, H., Wang, S., Yao, J., 2016. Photoelectrocatalytic reduction of perchlorate in aqueous solutions over Ag doped TiO2 nanotube arrays. J. Photochem. Photobiol. Chem. 328, 225–232. https://doi.org/10.1016/j.jphotochem.2016.05.023

Jiang, J., Oberdörster, G., Biswas, P., 2008. Characterization of size, surface charge, and agglomeration state of nanoparticle dispersions for toxicological studies. J. Nanoparticle Res. 11, 77–89. https://doi.org/10.1007/s11051-008-9446-4

Jordan, N., Foerstendorf, H., Weiß, S., Heim, K., Schild, D., Brendler, V., 2011. Sorption of selenium(VI) onto anatase: Macroscopic and microscopic characterization. Geochim. Cosmochim. Acta 75, 1519–1530. https://doi.org/10.1016/j.gca.2011.01.012

Kasap, S., Koughia, C., Berashevich, J., Johanson, R., Reznik, A., 2015. Charge transport in pure and stabilized amorphous selenium: re-examination of the density of states distribution in the mobility gap and the role of defects. J. Mater. Sci. Mater. Electron. 26, 4644–4658. https://doi.org/10.1007/s10854-015-3069-1

Kikuchi, E., Sakamoto, H., 2000. Kinetics of the Reduction Reaction of Selenate Ions by TiO2 Photocatalyst. J. Electrochem. Soc. 147, 4589–4593. https://doi.org/10.1149/1.1394106

Kot, A., Namieśnik, J., 2000. The role of speciation in analytical chemistry. TrAC Trends Anal. Chem. 19, 69–79. https://doi.org/10.1016/S0165-9936(99)00195-8

Labaran, B.A., Vohra, M.S., 2014. Photocatalytic removal of selenite and selenate species: effect of EDTA and other process variables. Environ. Technol. 35, 1091–1100. https://doi.org/10.1080/09593330.2013.861857

LeBlanc, K.L., Wallschläger, D., 2016. Production and Release of Selenomethionine and Related Organic Selenium Species by Microorganisms in Natural and Industrial Waters. Environ. Sci. Technol. 50, 6164–6171. https://doi.org/10.1021/acs.est.5b05315

Lenz, M., Hullebusch, E.D.V., Hommes, G., Corvini, P.F.X., Lens, P.N.L., 2008. Selenate removal in methanogenic and sulfate-reducing upflow anaerobic sludge bed reactors. Water Res. 42, 2184–2194. https://doi.org/10.1016/j.watres.2007.11.031

Leshuk, T., B. Holmes, A., Ranatunga, D., Z. Chen, P., Jiang, Y., Gu, F., 2018. Magnetic flocculation for nanoparticle separation and catalyst recycling. Environ. Sci. Nano 5, 509–519. https://doi.org/10.1039/C7EN00827A

Li, C., Cao, J., Ren, H., Li, Y., Tang, S., 2015. Comparison on kinetics and microbial community among denitrification process fed by different kinds of volatile fatty acids. Process Biochem. 50, 447–455. https://doi.org/10.1016/j.procbio.2015.01.005

Luek, A., Brock, C., Rowan, D.J., Rasmussen, J.B., 2014. A Simplified Anaerobic Bioreactor for the Treatment of Selenium-Laden Discharges from Non-acidic, End-Pit Lakes. Mine Water Environ. 33, 295–306. https://doi.org/10.1007/s10230-014-0296-2

Luiz, D. de B., Andersen, S.L.F., Berger, C., José, H.J., Moreira, R. de F.P.M., 2012. Photocatalytic reduction of nitrate ions in water over metal-modified TiO2. J. Photochem. Photobiol. Chem. 246, 36–44. https://doi.org/10.1016/j.jphotochem.2012.07.011

Mal, J., Nancharaiah, Y.V., van Hullebusch, E.D., Lens, P.N.L., 2017. Biological removal of selenate and ammonium by activated sludge in a sequencing batch reactor. Bioresour. Technol. 229, 11–19. https://doi.org/10.1016/j.biortech.2016.12.112

Mal, J., Nancharaiah, Y.V., van Hullebusch, E.D., Lens, P.N.L., 2016. Effect of heavy metal co-contaminants on selenite bioreduction by anaerobic granular sludge. Bioresour. Technol. 206, 1–8. https://doi.org/10.1016/j.biortech.2016.01.064

Marks, R., Yang, T., Westerhoff, P., Doudrick, K., 2016. Comparative analysis of the photocatalytic reduction of drinking water oxoanions using titanium dioxide. Water Res. 104, 11–19. https://doi.org/10.1016/j.watres.2016.07.052

Martin, A.J., Fraser, C., Simpson, S., Belzile, N., Chen, Y.-W., London, J., Wallschläger, D., 2018. Hydrological and biogeochemical controls governing the speciation and accumulation of selenium in a wetland influenced by mine drainage. Environ. Toxicol. Chem. 37, 1824–1838. https://doi.org/10.1002/etc.4123

Nakajima, T., Kamito, R., Takanashi, H., Ohki, A., 2013. Reduction of Selenate from Simulated Wet Flue Gas Desulfurization Wastewater Using Photocatalyst and Microorganism. J. Water Environ. Technol. 11, 419–427. https://doi.org/10.2965/jwet.2013.419

Nakajima, T., Yamada, K., Idehara, H., Takanashi, H., Ohki, A., 2011. Removal of Selenium (VI) from Simulated Wet Flue Gas Desulfurization Wastewater Using Photocatalytic Reduction. J. Water Environ. Technol. 9, 13–19. https://doi.org/10.2965/jwet.2011.13

Nancharaiah, Y.V., Lens, P.N.L., 2015. Ecology and Biotechnology of Selenium-Respiring Bacteria. Microbiol. Mol. Biol. Rev. 79, 61–80. https://doi.org/10.1128/MMBR.00037-14

Nguyen, V.N.H., Beydoun, D., Amal, R., 2005. Photocatalytic reduction of selenite and selenate using TiO2 photocatalyst. J. Photochem. Photobiol. Chem. 171, 113–120. https://doi.org/10.1016/j.jphotochem.2004.09.015

Ni, M., Leung, M.K.H., Leung, D.Y.C., Sumathy, K., 2007. A review and recent developments in photocatalytic water-splitting using TiO2 for hydrogen production. Renew. Sustain. Energy Rev. 11, 401–425. https://doi.org/10.1016/j.rser.2005.01.009

Nishimura, Y., Kamihara, T., Fukui, S., 1980. Diverse effects of formate on the dissimilatory metabolism of nitrate in Pseudomonas denitrificans ATCC 13867: Growth, nitrite accumulation in culture, cellular activities of nitrate and nitrite reductases. Arch. Microbiol. 124, 191–195. https://doi.org/10.1007/BF00427726

Nordstrom, D.K., Blowes, D.W., Ptacek, C.J., 2015. Hydrogeochemistry and microbiology of mine drainage: An update. Appl. Geochem., Environmental Geochemistry of Modern Mining 57, 3–16. https://doi.org/10.1016/j.apgeochem.2015.02.008

Pabby, A.K., Rizvi, S.S.H., Requena, A.M.S., 2008. Handbook of Membrane Separations: Chemical, Pharmaceutical, Food, and Biotechnological Applications. CRC Press.

Petty, J.T., Fulton, J.B., Strager, M.P., Merovich, G.T., Stiles, J.M., Ziemkiewicz, P.F., 2010. Landscape indicators and thresholds of stream ecological impairment in an intensively mined Appalachian watershed. J. North Am. Benthol. Soc. 29, 1292–1309. https://doi.org/10.1899/09-149.1

R. H. Gerber, A., 1986. The effect of acetate and other short-chain carbon compounds on the kinetics of biological nutrient removal. Water SA 12, 7–12.

Richards, L.A., Richards, B.S., Schäfer, A.I., 2011. Renewable energy powered membrane technology: Salt and inorganic contaminant removal by nanofiltration/reverse osmosis. J. Membr. Sci. 369, 188–195. https://doi.org/10.1016/j.memsci.2010.11.069

Rioja, N., Zorita, S., Peñas, F.J., 2016. Effect of water matrix on photocatalytic degradation and general kinetic modeling. Appl. Catal. B Environ. 180, 330–335. https://doi.org/10.1016/j.apcatb.2015.06.038

Rovira, M., Giménez, J., Martínez, M., Martínez-Lladó, X., de Pablo, J., Martí, V., Duro, L., 2008. Sorption of selenium(IV) and selenium(VI) onto natural iron oxides: Goethite and hematite. J. Hazard. Mater. 150, 279–284. https://doi.org/10.1016/j.jhazmat.2007.04.098

Santos, S., Ungureanu, G., Boaventura, R., Botelho, C., 2015. Selenium contaminated waters: An overview of analytical methods, treatment options and recent advances in sorption methods. Sci. Total Environ. 521–522, 246–260. https://doi.org/10.1016/j.scitotenv.2015.03.107

Sanuki, S., Arai, K., Kojima, T., Nagaoka, S., Majima, H., 1999. Photocatalytic reduction of selenate and selenite solutions using TiO2 powders. Metall. Mater. Trans. B 30, 15–20. https://doi.org/10.1007/s11663-999-0002-0

Schiavon, M., Pilon-Smits, E.A.H., 2017. Selenium Biofortification and Phytoremediation Phytotechnologies: A Review. J. Environ. Qual. 46, 10–19. https://doi.org/10.2134/jeq2016.09.0342

Shaban, Y.A., El Maradny, A.A., Al Farawati, R.K., 2016. Photocatalytic reduction of nitrate in seawater using C/TiO2 nanoparticles. J. Photochem. Photobiol. Chem. 328, 114–121. https://doi.org/10.1016/j.jphotochem.2016.05.018

Sheng, H., Li, Q., Ma, W., Ji, H., Chen, C., Zhao, J., 2013. Photocatalytic degradation of organic pollutants on surface anionized TiO2: Common effect of anions for high hole-availability by water. Appl. Catal. B Environ. 138–139, 212–218. https://doi.org/10.1016/j.apcatb.2013.03.001

Strong, P.J., McDonald, B., Gapes, D.J., 2011. Enhancing denitrification using a carbon supplement generated from the wet oxidation of waste activated sludge. Bioresour. Technol., Special Issue on Challenges in Environmental Science and Engineering, CESE-2010: Technological Advances in Waste Treatment for a Sustainable Future 102, 5533–5540. https://doi.org/10.1016/j.biortech.2010.12.025

Sun, D., Yang, W., Zhou, L., Sun, W., Li, Q., Shang, J.K., 2016. The selective deposition of silver nanoparticles onto {101} facets of TiO2 nanocrystals with co-exposed {001}/{101} facets, and their enhanced photocatalytic reduction of aqueous nitrate under simulated solar illumination. Appl. Catal. B Environ. 182, 85–93. https://doi.org/10.1016/j.apcatb.2015.09.005

Suttiponparnit, K., Jiang, J., Sahu, M., Suvachittanont, S., Charinpanitkul, T., Biswas, P., 2010. Role of Surface Area, Primary Particle Size, and Crystal Phase on Titanium Dioxide Nanoparticle Dispersion Properties. Nanoscale Res Lett 6, 27. https://doi.org/10.1007/s11671-010-9772-1

T. Tan, D.B., 2003. Effect of organic hole scavengers on the photocatalytic reduction of selenium ions. J. Photochem. Photobiol. Chem. 159, 273–280. https://doi.org/10.1016/S1010-6030(03)00171-0

Tan, L.C., Nancharaiah, Y.V., van Hullebusch, E.D., Lens, P.N.L., 2016. Selenium: environmental significance, pollution, and biological treatment technologies. Biotechnol. Adv. 34, 886–907. https://doi.org/10.1016/j.biotechadv.2016.05.005

Tan, T.T.Y., Beydoun, D., Amal, R., 2003a. Effects of organic hole scavengers on the photocatalytic reduction of selenium anions. J. Photochem. Photobiol. Chem. 159, 273–280. https://doi.org/10.1016/S1010-6030(03)00171-0

Tan, T.T.Y., Beydoun, D., Amal, R., 2003b. Photocatalytic reduction of Se(VI) in aqueous solutions in UV/TiO2 system: importance of optimum ratio of reactants on TiO2 surface. J. Mol. Catal. Chem. 202, 73–85. https://doi.org/10.1016/S1381-1169(03)00205-X

Turolla, A., Piazzoli, A., Farner Budarz, J., Wiesner, M.R., Antonelli, M., 2015. Experimental measurement and modelling of reactive species generation in TiO2 nanoparticle photocatalysis. Chem. Eng. J. 271, 260–268. https://doi.org/10.1016/j.cej.2015.03.004

Uden, P.C., 2002. Modern trends in the speciation of selenium by hyphenated techniques. Anal. Bioanal. Chem. 373, 422–431. https://doi.org/10.1007/s00216-002-1405-9

U.S. EPA, 2011. The Effects of Mountaintop Mines and Valley Fills on Aquatic Ecosystems of the Central Appalachian Coalfields (2011 Final).

U.S. EPA, 1996. EPA Method 3050B: Acid Digestion of Sediments, Sludges, and Soils.

Valari, M., Antoniadis, A., Mantzavinos, D., Poulios, I., 2015. Photocatalytic reduction of Cr(VI) over titania suspensions. Catal. Today, 8th European Meeting on Solar Chemistry and Photocatalysis: Environmental Applications 252, 190–194. https://doi.org/10.1016/j.cattod.2014.10.014

Watson, R.J., Butler, E.C.V., Clementson, L.A., Berry, K.M., 2005. Flow-injection analysis with fluorescence detection for the determination of trace levels of ammonium in seawater. J. Environ. Monit. 7, 37–42. https://doi.org/10.1039/B405924G

Xiao, Q., Yu, S., Li, L., Wang, T., Liao, X., Ye, Y., 2017. An overview of advanced reduction processes for bromate removal from drinking water: Reducing agents, activation methods, applications and mechanisms. J. Hazard. Mater. 324, 230–240. https://doi.org/10.1016/j.jhazmat.2016.10.053

Yang, T., Doudrick, K., Westerhoff, P., 2013. Photocatalytic reduction of nitrate using titanium dioxide for regeneration of ion exchange brine. Water Res. 47, 1299–1307. https://doi.org/10.1016/j.watres.2012.11.047